

DISCOVERY OF A THIRD HARMONIC CYCLOTRON RESONANCE SCATTERING FEATURE IN THE X-RAY SPECTRUM OF 4U 0115+63

W. A. HEINDL, W. COBURN, D. E. GRUBER, M. R. PELLING, AND R. E. ROTHSCHILD

Center for Astrophysics and Space Sciences, Code 0424, University of California, San Diego, La Jolla, CA 92093; wheindl@ucsd.edu

AND

J. WILMS, K. POTTSCHMIDT, AND R. STAUBERT

Institut für Astronomie und Astrophysik–Astronomie, University of Tübingen, Waldhäuser Strasse 64, D-72076 Tübingen, Germany

Received 1999 April 14; accepted 1999 June 8; published 1999 July 6

ABSTRACT

We have discovered a third harmonic cyclotron resonance scattering feature (CRSF) in observations of the recent outburst of 4U 0115+63 with the *Rossi X-Ray Timing Explorer (RXTE)*. The spectrum in a narrow pulse phase range shows CRSFs at $12.40^{+0.65}_{-0.35}$, $21.45^{+0.25}_{-0.38}$, and $33.56^{+0.70}_{-0.90}$ keV. With centroid energy ratios to the fundamental of 1.73 ± 0.08 and 2.71 ± 0.13 , the CRSFs are not harmonically spaced. Strong variability of the continuum and CRSFs with pulse phase indicate a complex emission geometry near the neutron star polar cap. In addition, one *RXTE* observation, which spanned periastron passage, revealed a strong 2 mHz quasi-periodic oscillation (QPO). This is slower by 2 orders of magnitude than the beat-frequency QPO expected in this system and slower by a factor of more than 5 compared with other QPOs seen in accreting X-ray pulsars.

Subject headings: stars: individual (4U 0115+63) — stars: neutron — X-rays: stars

1. INTRODUCTION

The transient X-ray source 4U 0115+63 is an accreting X-ray pulsar in an eccentric 24 day orbit (Bildsten et al. 1997) with the O9e star V635 Cassiopeiae (Unger et al. 1998). X-ray outbursts have been observed from 4U 0115+63 with *Uhuru* (Forman, Jones, & Tananbaum 1976), *HEAO 1* (Wheaton et al. 1979; Rose et al. 1979), *Ginga* (e.g., Tamura et al. 1992), and *CGRO/BATSE* (Bildsten et al. 1997).

A cyclotron resonance scattering feature (CRSF) in 4U 0115+63 was first noted near 20 keV by Wheaton et al. (1979) with the UCSD/MIT hard X-ray (10–100 keV) experiment aboard *HEAO 1*. White, Swank, & Holt (1983) analyzed concurrent data from the lower energy (2–50 keV) *HEAO 1/A-2* experiment and found an additional feature at ~ 12 keV. Two outbursts of 4U 0115+63 were observed with *Ginga*, in 1990 February and 1991 April (Nagase et al. 1991; Tamura et al. 1992; Mihara 1995). The pattern of absorption features differed dramatically in the two outbursts. A pair of features similar to the *HEAO 1* results in the 1990 outburst gave way to a single feature near 17 keV in 1991 (Mihara, Makishima, & Nagase 1998).

We discuss here spectral and timing analyses of observations of the 1999 March outburst (Wilson, Harmon, & Finger 1999; Heindl & Coburn 1999) obtained with the *Rossi X-Ray Timing Explorer (RXTE)*.

2. OBSERVATIONS AND ANALYSIS

Observations were made with the Proportional Counter Array (PCA; Jahoda et al. 1996) and High-Energy X-ray Timing Experiment (HEXTE; Rothschild et al. 1998) on board *RXTE*. The PCA is a set of five xenon proportional counters sensitive in the energy range 2–60 keV with a total effective area of ~ 7000 cm². HEXTE consists of two arrays of four NaI(Tl)/CsI(Na) phoswich scintillation counters (15–250 keV) totaling ~ 1600 cm². The HEXTE alternates between source and background fields in order to measure the background. The PCA and HEXTE fields of view are collimated to the same 1° FWHM region.

Beginning on 1999 March 3, daily, short (~ 1 ks) monitoring observations were carried out. In addition, we performed four long pointings (duration ~ 15 – 35 ks, labeled A–D in Fig. 1) to search for CRSFs. Observation B, on 1999 March 11.87–12.32, spanned periastron passage at March 11.95 (Bildsten et al. 1997). Figure 1 shows the *RXTE*/All-Sky Monitor (ASM; 1.5–12 keV) light curve of 4U 0115+63 together with the times of the pointed observations. In this Letter, we concentrate on observation B.

2.1. Spectral Analysis

The spectrum of 4U 0115+63 varies significantly with neutron star rotation phase (Nagase et al. 1991), making fits to the average spectrum difficult to interpret. In order to study the evolution of the spectrum through the pulse, we corrected photon arrival times to both the solar system and the binary system barycenters using the ephemeris of Bildsten et al. (1997). We then applied a Z^2 period search (Buccheri et al. 1983) to the HEXTE data to determine the pulse period. Figure 2 shows folded light curves derived from spectra in 50 pulse phase bins for observation B, where the period was 3.614512(33) s. The folded light curve has a sharp main peak, followed by a broader, softer second peak, similar to earlier reports (White et al. 1983; Bildsten et al. 1997). In searching for CRSFs, we followed the spectral analysis methods described in Kreykenbohm et al. (1998).

Because CRSFs at ~ 12 and ~ 22 keV are known in 4U 0115+63 (White et al. 1983; Nagase et al. 1991), we first concentrated on the HEXTE data in which higher harmonics might appear. We fit a “cutoff power law” (a power law times an exponential) to the HEXTE spectra in 20 phase bins. The reduced χ^2 of these fits ranged from 1.3 to 12.3 (62 degrees of freedom [dof]). Concentrated at the main pulse and through the rise and peak of the second, there were significant residuals resembling absorption features near 20–25 keV. In the fall of the second peak, residuals appeared between 30 and 40 keV. We then fit for an absorption feature near 20–25 keV, resulting in values of reduced χ^2 between 0.7 and 2.0 (59 dof). We used a simple Gaussian model for the optical depth profile. Fig-

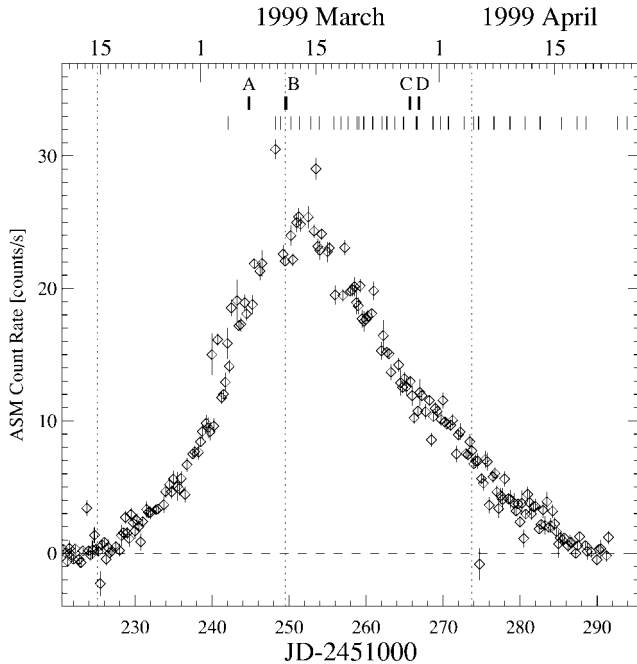


FIG. 1.—*RXTE*/ASM light curve of 4U 0115+63 averaged in 6 hr segments. The vertical dotted lines indicate times of periastron passage. The bars at the top indicate the times of the short, public *RXTE* pointings and of the long observations (heavy bars, A–D).

ure 2 shows the result of an F -test for adding this line. In the cases in which no line was allowed by the fit, the points are plotted with a value of 10^0 . Next, we allowed a CRSF between 28 and 45 keV. This significantly improved the fits in about half of the phase bins, including some near the main peak where large ~ 20 keV residuals in the initial fits masked the presence of this line. The corresponding F -test results are also plotted in Figure 2. Although there is strong evidence for multiple lines at other phases, the phase range 0.70–0.76 shared both a significant ~ 20 keV line as well as the most clearly linelike residuals in 30–40 keV in the no-lines fit. We therefore chose to concentrate on this phase in this Letter. We plan to perform detailed analysis of all phases and all four long (A–D) observations in a future paper.

Next, we jointly fit the HEXTE and PCA data for phase 0.70–0.76. To account for uncertainties in the response matrix, 1% systematic errors were applied to the PCA data. None of the continuum models (high-energy cutoff power law, Fermi-Dirac cutoff [FDCO] times a power law, and negative and positive power-law exponential [NPEX]; see Kreykenbohm et al. 1998) typically used for accreting pulsar spectra provided an acceptable fit without the inclusion of absorption features. A blackbody with $kT \sim 0.4$ keV and photoelectric absorption was required to describe the data. No Fe-K line was required. Ultimately, it was necessary to include CRSFs at ~ 12 , ~ 21 , and ~ 34 keV in the joint spectrum. The fitted line parameters were insensitive to the details of the continuum model used. The results given here used a FDCO times a power law, given by $F(E) \propto [1 + e^{(E-E_c)/E_f}]^{-1} E^{-\Gamma}$. F is the photon flux, E_c is the cutoff energy, E_f is the folding energy, and Γ is the photon index. E_c was fixed at zero. An F -test for the significance of adding the ~ 34 keV line to a model with only two absorption features gave a chance probability of 10^{-17} .

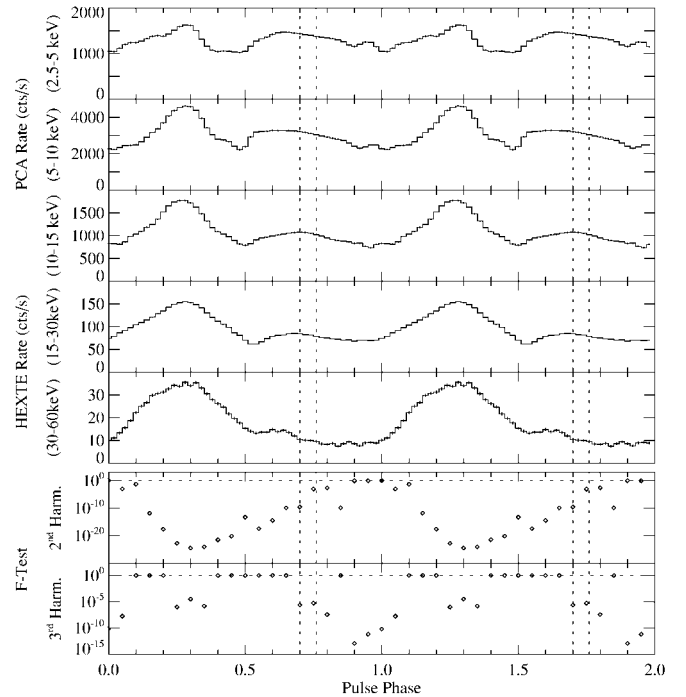


FIG. 2.—*Top*: *RXTE* folded light curve of 4U 0115+63 in five energy bands. *Bottom*: F -test probability for the addition of a second and subsequently a third CRSF to a simple continuum fit to the HEXTE data in 20 phase bins. In both panels, points which fall on the dashed line at 10^0 indicate no improvement of the fit for addition of that line. Vertical dotted lines delineate pulse phase 0.70–0.76 corresponding to the spectrum in Fig. 3.

2.2. Temporal Variability

Along with standard Fourier techniques, we analyzed the data in the time domain using the linear state space model (LSSM) formalism described by König & Timmer (1997) and Pottschmidt et al. (1998). Parameters of the LSSM are related to dynamical timescales of the system such as oscillation periods, decay times of damped oscillators, and stochastic noise. As shown in Figure 4, the data are well described by an LSSM of order 2. This model, based on an autoregressive process, is dominated by a stochastically driven sinusoid of period 552 s which exponentially decays with an e -folding time of $P_{\text{fold}} = 282$ s. This short P_{fold} accounts for the broad quasi-periodic oscillation (QPO) peak seen in the power spectral density (Fig. 5). A Kolmogoroff-Smirnoff test shows that the difference between the data and the LSSM is purely attributable to white noise. The light curve is thus consistent with a single exponentially decaying sinusoid, driven by a white noise process.

3. RESULTS AND DISCUSSION

3.1. Spectrum and CRSFs

Figure 3 shows the best-fit joint count spectrum from pulse phase 0.70–0.76. Also plotted is the inferred incident photon spectrum. Best-fit parameters are given in Table 1, and the reduced χ^2 of the fit is 1.66 (74 dof). This is the first time that a fundamental and two harmonic CRSFs have been detected in a single accreting X-ray pulsar spectrum. Previously, at most a fundamental and second harmonic have been seen (4U 1907+09 [Cusumano et al. 1998] or suggested (Vela X-1 [Kreykenbohm et al. 1998], A0535+25 [Kendziorra et al.

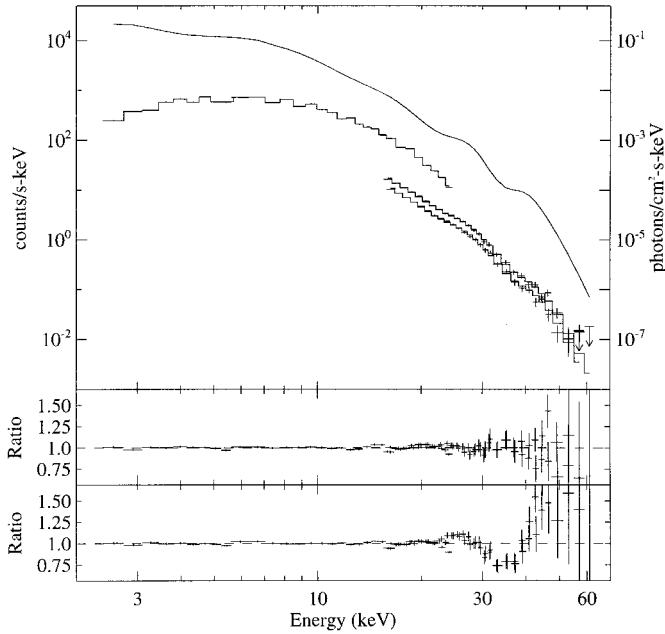


Fig. 3.—*Top*: PCA and HEXTE count spectra (*plus signs*) for pulse phase 0.70–0.76. Also shown are the best-fit model (*histograms*) with three CRSFs and the inferred incident spectrum (*smooth curve*). *Middle*: Ratio of the data to the best-fit model. *Bottom*: Ratio of the data to a model fit with only two CRSFs. The residuals between 30–40 keV and the underprediction of the continuum above 40 keV emphasize the presence of the third line.

1994], and 1E 2259+586 [Iwasawa, Koyama, & Halpern 1992]). Those earlier observations lacked the broadband sensitivity of *RXTE*. Furthermore, simple fits to the phase-resolved HEXTE spectra show that the X-ray spectrum varies rapidly with neutron star rotation. We observe significant variations between consecutive phase bins which cover only 2% of the pulse phase. This suggests complex spatial variations of conditions near the neutron star polar cap. Since the 35 keV CRSF is only present in about half of the pulse (predominantly during the fall of the second, weaker pulse) and both the 22 and 35 keV lines are only present together in three of 20 coarse phase bins, averaging over large phase angles would likely have washed out the line in the variable continuum.

The fundamental energy of 12.4 keV implies a neutron star surface field of $1.1 \times 10^{12}(1+z)$ G. Contrary to simple Landau theory, the observed line spacing is not quite harmonic. The ratio of the second and third harmonics to the fundamental are 1.73 ± 0.08 and 2.71 ± 0.13 , respectively. We tried fits with the second and third lines constrained to be exact harmonics of the first, whose energy was allowed to vary. The resulting fit was unacceptable (reduced χ^2 of 6.7 with 76 dof). We did, however, find a reasonable fit with the third harmonic tied to the first but the second free to vary. Nevertheless, an *F*-test comparing this fit to our best model gives a chance improvement probability of 2×10^{-4} for allowing the non-integer energy ratio of the first and third lines.

In addition to relativistic shifts, line energies may deviate from harmonic for a number of reasons. The main scattering for the harmonics may take place in regions of different magnetic field, either resulting from optical depth effects in the mound of accreting matter or for lines primarily produced at opposite magnetic poles. It is interesting to note (see Fig. 2) that the second and third harmonics are most significant in the

TABLE 1
PARAMETERS OF THE BEST-FIT MODEL SPECTRUM (SEE § 2.1)

Harmonic	Energy (keV)	Width ^a (keV)	Optical Depth
1 (fundamental)	$12.40^{+0.65}_{-0.35}$	$3.3^{+1.9}_{-0.4}$	$0.72^{+0.10}_{-0.17}$
2	$21.45^{+0.25}_{-0.38}$	$4.5^{+0.7}_{-0.9}$	$1.24^{+0.04}_{-0.06}$
3	$33.56^{+0.70}_{-0.90}$	$3.8^{+1.5}_{-0.9}$	$1.01^{+0.13}_{-0.14}$

^a One standard deviation of the Gaussian optical depth profile.

main and secondary pulses, respectively, possibly indicating origins at opposite poles.

In our initial fits to the HEXTE data alone, we observed that the 20 keV CRSF varied in both strength and energy (by 20%) through the pulse phase. This was first observed with *Ginga* by Nagase et al. (1991) in the 1990 February outburst. The line is strongest and the energy highest (~ 24 keV) on the falling edge of the main pulse, which is similar to the behavior of the CRSFs in Cen X-3 and 4U 1626–67 (Heindl & Chakrabarty 1999). The *Ginga* data showed significant ~ 11 and ~ 22 keV lines at all eight pulse phases analyzed (Mihara 1995). The HEXTE data find that the ~ 20 keV line is not required just before the rise of the main pulse (Fig. 2). However, with the addition of the PCA data, which constrain the continuum and fundamental line, it is possible that this line will be required at all phases. In any case, strong long-term variability of the lines is known (Mihara 1995), so differences between these results and earlier observations are not surprising.

3.2. Temporal Variability: A 2 mHz QPO

Figures 4 and 5 show the PCA light curve of observation B and its power spectral density (PSD), respectively. Strong variability with an ~ 500 s period is obvious. At frequencies above 5 mHz, the PSD can be described by an overall power law $\propto f^{-1}$ plus peaks at the neutron star rotational frequency and its multiples. Some accreting pulsars have shown a QPO at the beat frequency between the neutron star rotation and the Keplerian orbit at the inner edge of the accretion disk (Finger, Wilson, & Harmon 1996). Using the relations in Finger et al. (1996) with a surface magnetic field strength of 1.3×10^{12} G, a distance of 6 kpc (I. Negueruela 1999, private communication), and a total flux of 2.1×10^{-8} ergs cm^{-2} s^{-1} , the expected beat QPO frequency is 0.8 Hz. Overtones of the rotational

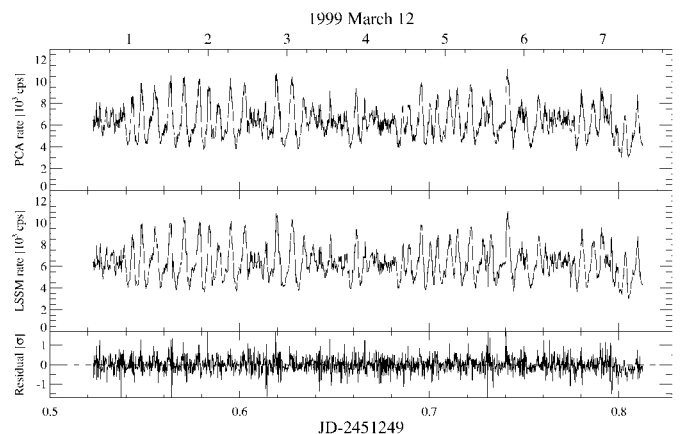


Fig. 4.—PCA (1.5–60 keV) light curve in 16 s bins of observation B together with a second-order linear state space model of the variability. The bottom panel shows the residuals of the LSSM.

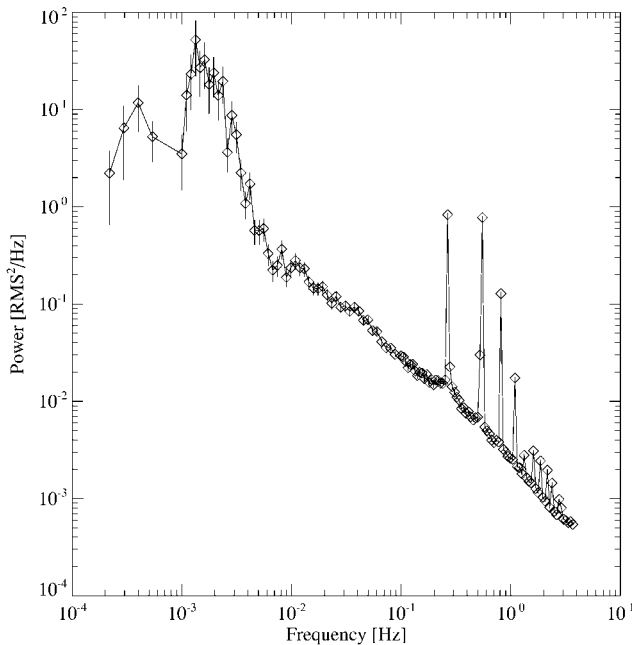


FIG. 5.—PSD (normalized according to Miyamoto et al. 1991) of the observation B PCA light curve. The PSD has been rebinned such that $dff = 0.35, 0.1$, and 0.05 in the frequency bands 10^{-4} – 10^{-3} , 10^{-3} – 10^{-1} , and 10^{-1} – 10^1 Hz, respectively. The ~ 2 mHz QPO and several harmonics of the 3.6 s pulsation are clear above a $1/f$ continuum.

frequency confuse the search for QPOs in this region (see Fig. 5), and no obvious peaks apart from the pulsation were seen in the 1 ks short pointings or in observation B.

Below 5 mHz, the PSD is dominated by a broad QPO feature from the 500 s oscillation. The shape of this feature is complex and asymmetric; it can be described neither by a Lorentzian line nor by the superposition of two Lorentzian lines. The feature peaks at ~ 1.5 mHz and has an FWHM of 1 mHz ($Q = f_0/\Delta f \approx 1.5$). The excess power of the QPO with respect to the underlying red noise component in the range from 1 to 4 mHz is $\sim 5\%$ rms. The ~ 500 s period of this oscillation is longer than any X-ray QPO previously reported in an accreting X-ray pulsar. Soong & Swank (1989) reported a broad 0.062 Hz QPO in *HEAO 1* observations of a flaring state in 4U 0115+63 that also did not fit into the beat frequency model.

The QPO was probably present in several of the short (~ 1 ks) observations as well, since there was apparent, slow variability on a several hundred second timescale. In observation A, the QPO was at most present weakly, since no clear peak is evident in the PSD. Two possible explanations for the QPO are (1) modulation of the accretion flow and (2) occultation of the beam by intervening matter in an accretion disk.

It seems unlikely that the variability is due to modulation of the accretion flow itself. The timescales at the neutron star pole (milliseconds) and the inner edge of the disk (seconds) are too fast. Furthermore, the rotation period (days) of V635 Cas is too long.

We compared PCA spectra at minima of the 500 s cycle to the spectra of the following maxima. The spectral shape is unchanged from 2.5 to 5 keV, and only $\sim 20\%$ deviations appear at higher energies. Because the spectrum below 5 keV is steady through the QPO and the flux varies by a factor of 2 from peak to minimum, the QPO mechanism cannot be absorption in *cold* material. If it were, the low-energy spectrum would be highly modified by photoelectric absorption. It is possible that Thomson scattering in ionized matter causes the variability. We suggest two possible mechanisms, which both require that the accretion disk be viewed nearly edge on. Both are consistent with a second-order LSSM process. First, an azimuthal warp propagating around the disk could cause the ionized disk surface to intervene in the line of sight. In this case, the 500 s timescale is the time for the wave to circle the disk (assuming a single-peaked warp). In the second picture, the absorption takes place in a lump in the disk which orbits at a Kepler period of 500 s.

4. SUMMARY

We have made two discoveries in the *RXTE* observations of the 1999 March outburst of 4U 0115+63. The *HEXTE* data have revealed for the first time in any pulsar a third harmonic CRSF. The line spacing between the fundamental and second harmonic and between the second and third harmonics are not equal and are not multiples of the fundamental line energy. We have also discovered the slowest (2 mHz) QPO yet observed from an accreting pulsar. It was most pronounced during an observation spanning periastron passage of the neutron star around its massive companion. Based on the timescale, amplitude, and energy spectrum of the oscillation, it is most likely due to obscuration of the neutron star by hot accretion disk matter. The longest QPO previously observed had a timescale of 100 s in SMC X-1 (Angelini, Stella, & White 1991).

We thank E. Smith, J. Swank, and C. Williams-Heikkilä for rapidly scheduling the observations and supplying the real-time data. *ASM* data are provided by the *RXTE/ASM* teams at Massachusetts Institute of Technology and at the *RXTE* Science Operations Facility and Guest Observer Facility at NASA's Goddard Space Flight Center. We also thank the anonymous referee for very useful comments and suggestions. This work was supported by NASA grants NAS5-30720 and NAG5-7339, Deutsche Forschungsgemeinschaft grant Sta 173/22, and a travel grant from the Deutscher Akademischer Austauschdienst.

REFERENCES

- Angelini, L., Stella, L., & White, N. E. 1991, *ApJ*, 371, 332
 Bildsten, L., et al. 1997, *ApJS*, 113, 367
 Buccheri, R., et al. 1983, *A&A*, 128, 245
 Cusumano, G., Di Salvo, T., Orlandini, M., Piraino, S., Robba, N., & Santangelo, A. 1998, *A&A*, 338, L79
 Finger, M., Wilson, R., & Harmon, B. 1996, *ApJ*, 459, 288
 Forman, W., Jones, C., & Tananbaum, H. 1976, *ApJ*, 206, L29
 Heindl, W., & Chakrabarty, D. 1999, in *MPE Rep., Highlights in X-ray Astronomy in Honour of Joachim Trümper's 65th Birthday* (Garching: MPE), in press
 Heindl, W., & Coburn, W. 1999, *IAU Circ.* 7126
 Iwasawa, K., Koyama, K., & Halpern, J. 1992, *PASJ*, 44, 9
 Jahoda, K., Swank, J. H., Giles, A. B., Stark, M. J., Strohmayer, T., & Zhang, W. 1996, *Proc. SPIE*, 2808, 59
 Kendziorra, E., et al. 1994, *A&A*, 291, L31
 König, M., & Timmer, J. 1997, *A&AS*, 124, 589
 Kreykenbohm, I., Kretschmar, P., Wilms, J., Staubert, R., Kendziorra, E., Gruber, D., Heindl, W., & Rothschild, R. 1998, *A&A*, 341, 141
 Mihara, T. 1995, Ph.D. thesis, Univ. Tokyo
 Mihara, T., Makishima, K., & Nagase, F. 1998, *Adv. Space Res.*, 22, 987

- Miyamoto, S., et al. 1991, ApJ, 383, 784
Nagase, N., et al. 1991, ApJ, 375, L49
Pottschmidt, K., König, M., Wilms, J., & Staubert, R. 1998, A&A, 334, 201
Rose, L., Pravdo, S., Kaluzienski, L., Marshall, F., Holt, S., Boldt, E., Rothschild, R., & Serlemitsos, P. 1979, ApJ, 231, 919
Rothschild, R., et al. 1998, ApJ, 496, 538
Soong, Y., & Swank, J. H. 1989, in Proc. 23rd ESLAB Symp. on Two Topics in X-Ray Astronomy, ed. N. White (ESA SP-296; Bologna: ESA), 617
Tamura, K., Tsunemi, H., Kitamoto, S., Hayashida, K., & Nagase, F. 1992, ApJ, 389, 676
Unger, S., Roche, P., Negueruela, I., Ringwald, F., Lloyd, C., & Coe, M. 1998, A&A, 336, 960
Wheaton, W. A., et al. 1979, Nature, 282, 240
White, N., Swank, J., & Holt, S. 1983, ApJ, 270, 711
Wilson, R., Harmon, B., & Finger, M. 1999, IAU Circ. 7116